Ultrasonics 94 (2019) 37–49

Contents lists available at ScienceDirect

Ultrasonics

journal homepage: www.elsevier.com/locate/ultras

Influence of volumic fraction of adhesive in elastic and viscous thin bonded Aluminum/Adhesive/Aluminum plate on Lamb modes that have ZGV modes

Souhail Dahmen

Laboratory of Physics of Materials, Faculty of Sciences of Sfax, University of Sfax, PB 815, 3018 Sfax, Tunisia

ARTICLE INFO

Keyword:
Lamb waves
Viscous thin bonded plate
Backward mode
Dispersion and attenuation curves
ZGV mode
Coupling mode

ABSTRACT

Before a nondestructive testing process gets set up, the sensitivity of the Lamb waves to the bonded plate's properties must be well understood. The dispersion and attenuation curves in thin bonded Aluminum/Adhesive/Aluminum plate are calculated by the Stiffness matrix method. The increase in the volumic fraction d caused the appearance of backward mode in the S_0 and S_2 dispersion curves. The effect of d on forward waves, and on backward waves and associated ZGV-modes, are studied. The frequencies of ZGV-modes decrease when d increases. The effects of d on dispersion and attenuation curves of the damped symmetric modes are shown. From certain values of d, and at the frequencies of the ZGV-modes, the dispersion curves of the symmetric modes are connected. This phenomenon gives rise to a C coupling mode. The attenuation levels of the ZGV-modes for different d values are calculated. The increase in d caused the shift of C-dispersion and C-attenuation curves toward the decreasing direction of the frequency axis, without significant change in the values of the phase velocity, and with slight decreases in the attenuation level of the C coupling mode.

1. Introduction

The bonded plates made of two materials an adhesive layer in between are increasingly used in the modern aerospace and automobile industries [1]. This increasing use of adhesive bonding in the industry has been motivated by the need of stronger and lighter structures. For that reason, it is interesting to estimate the bonding conditions such as the thickness of the layer and bond strength for ensuring the integrity of the technology. Usually the adhesive bond layer itself is not accessible or visible. The choice of Lamb waves for testing such structures has been motivated due to their great potentiality for quickly testing quite a long range of the specimen. Large areas of plate structures can be inspected and monitored from a single, remote access point using guided ultrasonic waves [2]. These are often used in a low frequency-thickness range below the cut-off frequency of the higher wave modes to simplify data interpretation [3]. However, the resulting wavelengths are typically significantly larger than in bulk wave UT, thus limiting the sensitivity for the detection of small defects [4]. However, in high frequency guided ultrasonic waves are attenuated, if a material, such as an adhesive, is present between the metallic layers, making the monitoring of large areas more difficult. The potential of high frequency guided waves for hidden defect detection at critical and difficult to access locations in uniform multilayer component consists of two aluminums plates with a sealant layer, in bonded plate model aerospace structures has been investigated [5].

Some recent works have been shown that zero-group velocity (ZGV) Lamb modes, allow a local measurement of mechanical properties of sandwich bonded plates [6]. These local ZGV resonances have been used in to image the lack of adhesive bond between two plates [7]. The experiments were carried out on a 0.5 mm thick Duralumin plate bonded with a 0.2 mm thick epoxy layer to a 2 mm thick glass plate. In the centre, an air bubble was imprisoned. The amplitude of the resonance S_1-ZGV Lamb mode is measured in different points around the disbanded area. Therefore, change in the level of attenuation of the resonance S_1-ZGV Lamb mode with the thickness of the epoxy layer, gives a valuable information with a large contrast on adhesive disbanded. In additional, they demonstrated the ability of this technique to detect a very small change in the micrometric adhesive layer. They have bonded a 0.5-mm thick Duralumin plate to a 1.08 mm thick glass plate with a variable thin layer of cyanilite. The thickness varies from 0 to 40 μm over a distance of 60 mm. they found that the frequency of ZGV mode decreases linearly with the thickness glue increase. Moreover, around the S_1-ZGV Lamb mode resonance, they observe multiple resonances whose variations in amplitude are thickness joint dependent. H Cho1 and all, used this technique to characterize the thickness of an adhesive epoxy layer sandwiched between different materials and the bond quality for brazed material using a laser ultrasonic technique. Using two modes of the ZGV Lamb modes, the thickness of the adhesive

E-mail address: souhail.dahmen@yahoo.fr.

https://doi.org/10.1016/j.ultras.2018.12.005
Received 23 August 2018; Received in revised form 7 December 2018; Accepted 10 December 2018
Available online 11 December 2018
0041-624X/

layer ranging from 0.2 to 0.8 mm can be estimated with high accuracy [8]. In order to understand the existence and the frequency response in the bonded plate, numerical calculations of dispersion curves including bonded plate had been performed [9,10]. Recently, a non contact method based on the measurement of ZGV resonance frequencies was proposed to probe interfacial stiffness between two plates [11]. An interfacial behavior model [12,13] was used to calculate the dispersion curves and zero-group velocity Lamb modes in a symmetrical structure composed of two plates coupled with a thin layer. They propose a numerical study of the dependence of ZGV modes on the bonding layer thickness and on the interfacial stiffnesses. Provided the bonding layer thickness is well known, the low frequency ZGV Lamb mode was used to estimate the normal stiffness and the first anti-symmetrical ZGV Lamb mode used to estimate the normal stiffness. Difference between theoretical and the other experimental ZGV frequencies was found to be less than 0.3% which shows the potential interest of this technique [14].

In addition to the simple ZGV mode, the dispersion curve of certain modes in some materials can exhibit two or three ZGV modes. Some works have been reported the ability of this multiple ZGV modes in the nondestructive control domain. M. V. Predoi reported the multiple ZGV modes of Lamb modes in multilayered pipes [15]. The phenomenon of double ZGV modes has been found in a fluid-filled thin-walled pipe which used in the civil and energy industries, and hence need to be inspected regularly to certify their safety and reliability [16]. Cui et al. have studied the influence of the contained liquid on backward waves and associated ZGV modes, in order to explore whether this ZGV technique is suitable for in-service non-destructive evaluations of liquid-filled pipes [17]. In 2012, Hussain and Ahmad reported the multiple ZGV modes in an orthotropic plate [18]. They found that all symmetric modes beyond S_{16} and antisymmetric modes beyond A_{25} possess one or more ZGV points. Unlike in the well studied case of "backward traveling" Lamb waves in plates, Maznev et al. found that this anomalous behavior is exhibited by the lowest acoustic mode of a thin film structure on silicon substrate [19]. The measurements were performed on a silicon substrate coated with multilayer stack. This multilayer structure, comprised of a spin-coated SiLK polymer14 with the thickness of 1.1 μm, Ta diffusion barrier layer with the thickness of 25 nm, and layer of copper Cu with the thickness of 100 nm. The dispersion curve of the lowest-mode exhibits two ZGV modes in both experimental data and simulations. This phenomenon of double ZGV modes does not have a direct free plate analogy, as in the latter case the three lowest modes (A_0, S_0 and A_1) never exhibit negative group velocity. Indeed, along such structure the guided modes propagation were little different than classical Lamb modes, because this multilayer is not free, contrary to most of composite material plates.

Among the objectives of this work, is to report this phenomenon of double ZGV modes for the fundamental mode in certain types of free multilayer plates. Then, study the impact of the change of the properties of the layers on the dispersion and attenuation curves of the Lamb waves around the frequency of the ZGV mode. To highlighting this phenomenon in bonded plate we have chosen the thin symmetric Aluminum/Adhesive/Aluminum plate used in Ref. [1]. The thin symmetric plate consists of two aluminum plates bonded together by a viscoelastic adhesive layer Fig. 1(a). It is characterized by a strong acoustic impedance contrast between their layers. In Ref. [1], Hong-Xiang et al. studied the generation of waves of lamb in this model of aerospace structures, subjected to laser illumination. The sensitivity of the signal to the variation of the thickness h of the viscoelastic adhesive layer in a three-layer plate with Aluminum/Adhesive/Aluminum configuration has been studied. In the study, the volume ratio of the adhesive was varied from 10% to 30% in a thin plate having a thickness of 100 μm. These results motivate our interest in studying the effect of the ratio volumic of the adhesive on the dispersive curves of lamb waves in this thin symmetric bonded plate. We found that, in addition to the conventional ZGV modes corresponding to the high modes, the

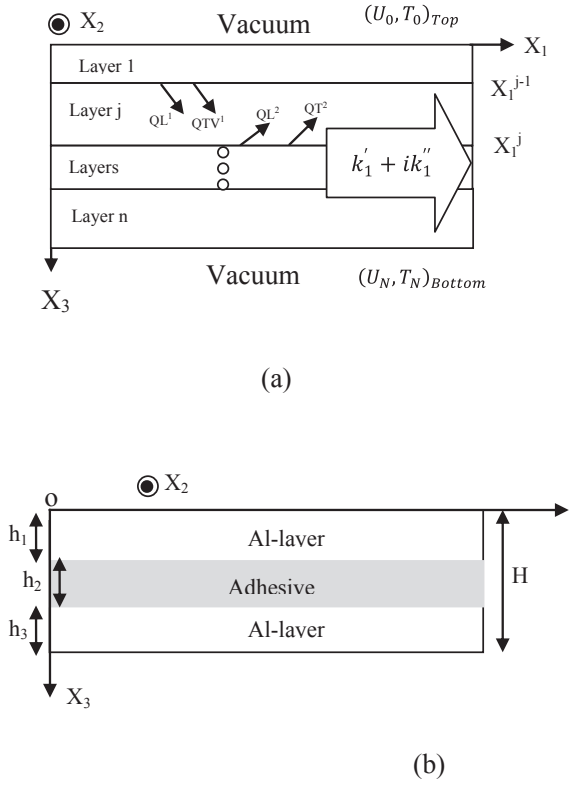

Fig. 1. (a) A schematic diagram of a n-layer plate, showing the coordinate system; (b) Schematic of three-layer bonded plate of two aluminum plates joined together with an adhesive bonding layer. The total thickness of the plate is H = 100 μm. the thickness of each aluminum layer is $h_1 = h_3$; thickness of adhesive layer is h_2; the volumic fraction of the bonded plate is defined by $d = 100\, h_2/H$.

spectrum of fundamental mode S_0 may be exhibit two ZGV modes.

In the literature, there are many analytical methods to solve the dispersion equation in the multilayer plate, such as the transfer matrix method [20,21], the global matrix method [22,23]. In 2003 the Stiffness matrix method was developed by Wang and Rokhlin [24,25]. It seems that this method is the most stable analytical method, which allows the determination of the dispersion curves. In this work we used the Stiffness matrix method to obtain the dispersion and attenuation curves of the guided wave in viscous Aluminum/Adhesive/Aluminum plate, which characterized by the strongly different acoustic impedances between their layers.

The first part of this work has been devoted to study the effects of change of the middle layer thickness on some dispersion curves of Lamb waves which exhibit ZGV mode. And thereby to investigate whether they can be use for in-service inspection of free sandwich structures. At the beginning, we report the existence of two ZGV modes for the fundamental symmetrical Lamb mode S_0 in the thin symmetric bonded plate Aluminum/Adhesive/Aluminum. The influence of the volumic fraction of adhesive on the frequency of ZGV mode is investigated.

Before a nondestructive testing process gets set up, the sensitivity of the Lamb waves to the bonded plate's properties must be well understood. In this work, we have chosen to investigate the influence of thickness layers changes on the three lowest symmetric modes S_0, S_1 and S_2 which their spectrums can exhibit ZGV modes.

The study was carried out when the total thickness of the plate remain constant. As in the case of the study carried out for the bonded plate in Ref. [1], the thickness of the intermediate layer and the thicknesses of two metallic layers changes, so that the plate remains symmetrical, and its total thickness remains equal to the standard value

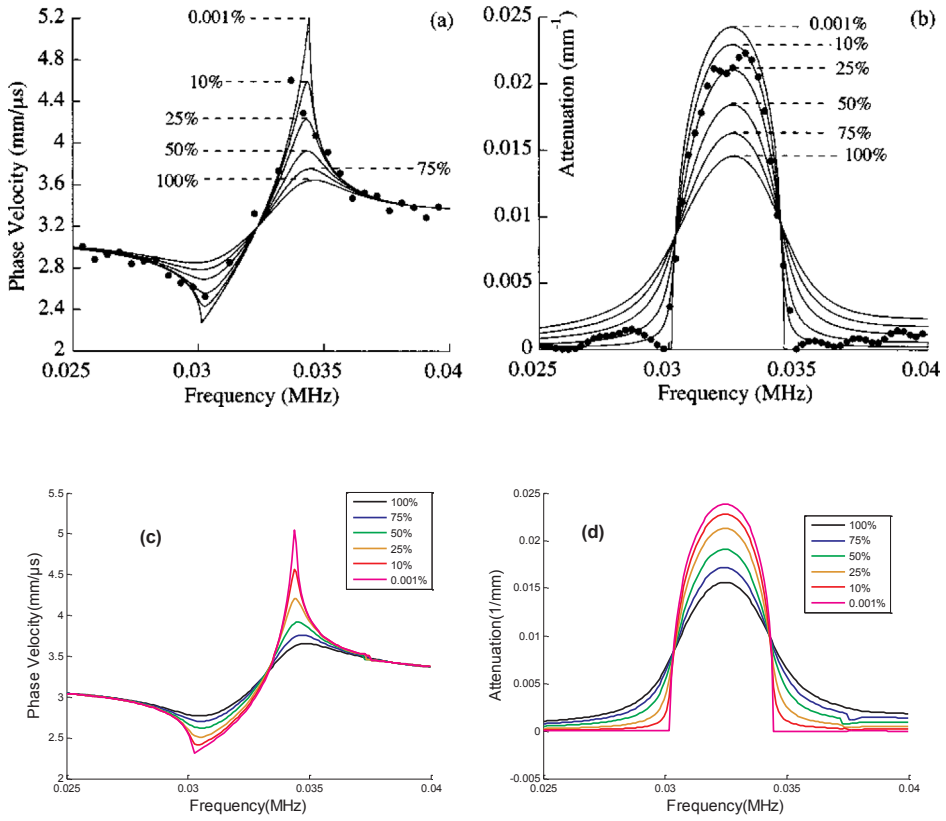

Fig. 2. Comparison of the complex solutions for sandwich plate calculated by: (c and d) the author's programs by using the Stiffness matrix method and (a and b) the Castaings's results calculated by Transfer matrix method.

(H = 100 μm) given in Ref. [1]. Finally, the viscous property of the adhesive layer is taken into account. The effects of the viscoelasticity on the dispersion curves which exhibit ZGV modes are investigated. The influences of the change of the adhesive layer thickness on these damped modes are discussed.

2. Mathematics and problem formulation

The model used for predicting the dispersion curves of guided modes is based on the Stifness matrix method. Let us consider a multilayered plate, consisting of N arbitrarily anisotropic and viscoelastic layers as illustrated in Fig. 1(a). The direction of propagation chosen here is direction x_1, so the plane of propagation is plane P_{13} formed by the pair of (x_1,x_3). Assuming that the wave propagation in the multilayered in terms of time is harmonic, the stress–strain equations of viscoelastic layer are similar to those in elastic layer, except that material properties of viscoelastic layer are complex numbers [26]. As shown in Fig. 1(a), the two components of total displacement vector, in the jth layer, may be written as the summation of four partial waves:

$$U_1^j = (A_{QL1}^j P_{1,QL1}^j e^{K_{3,QL1}^j (x_3 - x_3^{j-1})} + A_{QT1}^j P_{1,QT1}^j e^{K_{3,QT1}^j (x_3 - x_3^{j-1})} + A_{QL2}^j P_{1,QL2}^j e^{K_{3,QL2}^j (x_3 - x_3^j)} + A_{QT2}^j P_{1,QT2}^j e^{K_{3,QT2}^j (x_3 - j)}) e^{j(wt - K_1' X_1)} e^{-K_1'' X_1} \quad (1)$$

$$U_3^j = (A_{QL1}^j P_{3,QL1}^j e^{K_{3,QL1}^j (x_3 - x_3^{j-1})} + A_{QT1}^j P_{3,QT1}^j e^{K_{3,QT1}^j (x_3 - x_3^{j-1})} + A_{QL2}^j P_{3,QL2}^j e^{K_{3,QL2}^j (x_3 - x_3^j)} + A_{QT2}^j P_{3,QT2}^j e^{K_{3,QT2}^j (x_3 - j)}) e^{j(wt - K_1' X_1)} e^{-K_1'' X_1} \quad (2)$$

where A^j is the amplitude complexe, P^j is the unit displacement polarization vectors, and K_3^j is the x_3-component wave number. They are the characteristic of the four partial downward (QL1 and QT1) and upward (QL2 and QT2) traveling plane waves in the jth layer. K_1' is the wave number and K_1'' is the attenuation coefficient of the Lamb wave; with $K_1' = \frac{w}{V} = 2\pi/\lambda$: w is the impulsion (w = 2πf; f is the frequency), and λ and V are the wavelength and the phase velocity of the Lamb wave.

The stress component vector $T_j = (T_{31}^j, T_{33}^j)$ can be related to each of the plane wave displacement field using Hook's law:

$$T_{13}^j = (A_{QL1}^j D_{3,QL1}^j e^{K_{3,QL1}^j (x_3 - x_3^{j-1})} + A_{QT1}^j D_{3,QT1}^j e^{K_{3,QT1}^j (x_3 - x_3^{j-1})} + A_{QL2}^j D_{3,QL2}^j e^{K_{3,QL2}^j (x_3 - x_3^j)} + A_{QT2}^j D_{3,QT2}^j e^{K_{3,QT2}^j (x_3 - j)}) e^{j(wt - K_1' X_1)} e^{-K_1'' X_1} \quad (3)$$

$$T_{33}^j = (A_{QL1}^j D_{3,QL1}^j e^{K_{3,QL1}^j (x_3 - x_3^{j-1})} + A_{QT1}^j D_{3,QT1}^j e^{K_{3,QT1}^j (x_3 - x_3^{j-1})} + A_{QL2}^j D_{3,QL2}^j e^{K_{3,QL2}^j (x_3 - x_3^j)} + A_{QT2}^j D_{3,QT2}^j e^{K_{3,QT2}^j (x_3 - j)}) e^{j(wt - K_1' X_1)} e^{-K_1'' X_1} \quad (4)$$

where the components $D_{1,\mu}^j$ ($\mu \equiv QL1, QL2, QT1 or QT2$) are related to the polarization $P_{1,\mu}^j$ by $D_{i,\mu}^j = (C_{i3kl})^j P_{1,\mu}^j$. The coefficients $C_{ijkl} = C_{ijkl}' + jC_{ijkl}''$ of the layer stiffness matrix are complex where C_{ijkl}' represents the material stiffness, and C_{ijkl}'' the material viscosity. The displacement polarization P_k and wave numbers K are determined by solving the Christoffel equation: $(C_{ijkl} k_j k_l - \rho w^2 \delta_{il}) P_l = 0$, where ρ is the density.

A stiffness matrix that links the displacements U and stresses T, on the upper (u_j^+, T_j^+) and lower (u_j^-, T_j^-) interfaces bounding layer j, is written according to the following relation [24,25]:

$$\begin{bmatrix} T_3^- \\ T_5^- \\ T_3^+ \\ T_5^+ \end{bmatrix} = \begin{bmatrix} A_{11} & A_{12} & A_{13} & A_{14} \\ A_{21} & A_{22} & A_{23} & A_{24} \\ A_{31} & A_{32} & A_{33} & A_{33} \\ A_{41} & A_{42} & A_{43} & A_{44} \end{bmatrix} \begin{bmatrix} U_1^- \\ U_3^- \\ U_1^+ \\ U_3^+ \end{bmatrix} \quad (5)$$

Using the usual contracted notation for indices [24], i.e., $T_3 = T_{33}$ and $T = T_{13}$. The routine for calculating the elements of the stiffness matrix

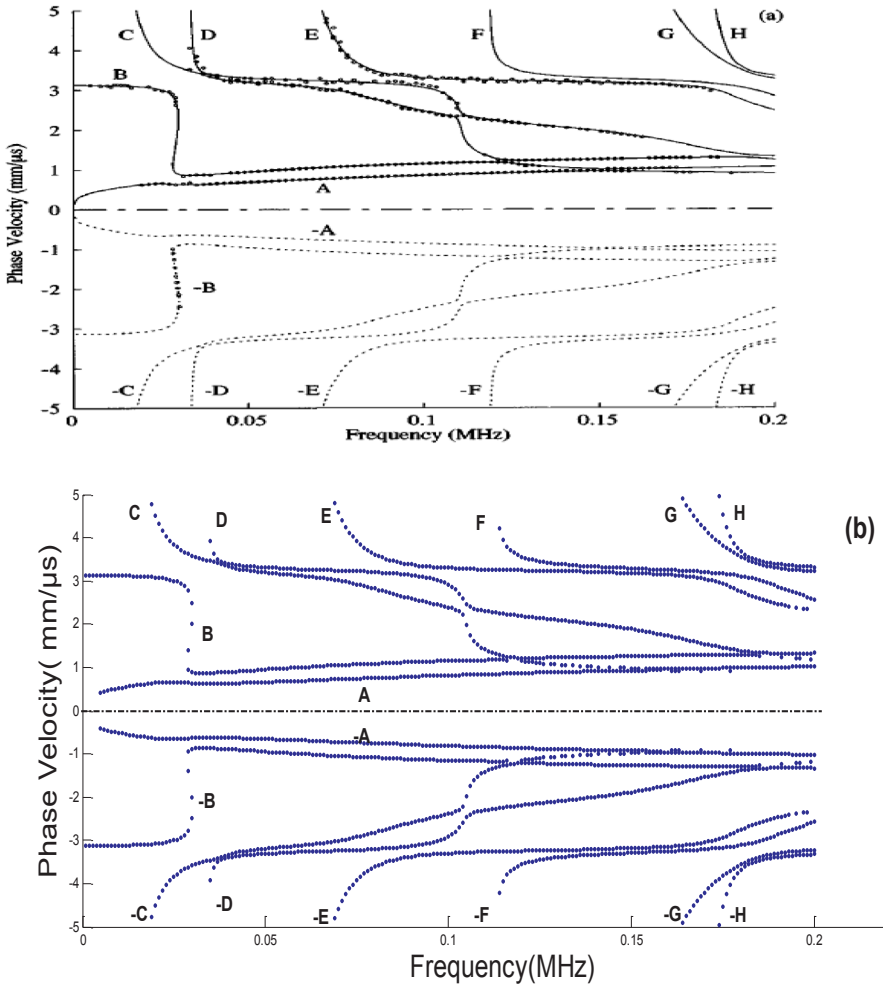

Fig. 3. Comparison of real solutions (positive phase velocity of A, B, C, D, E, F, G, H modes) and (negative phase velocity: -A, -B,- C, -D, -E, -F, -G, -H) for elastic sandwich plate calculated by: (b) the author's programs by using the Stiffness matrix method and (a) the Castaings's results.

Table1
Mechanical properties of materials' plate aluminum/adhesive/aluminum.

	Density (kg m^{-3})	C_{11} (GPa)	C_{33} (GPa)	C_{13} (GPa)	C_{55} (GPa)
Aluminum	2780	112	112	58	27
Adhesive	1100	7 + i0.21	7 + i0.21	4.8 + i0.144	1.1 + i0.033

$A_{pq}(p, q = 1, 2, 3, 4, 5, 6)$ is given in Ref. [20]. The boundary conditions at the internal solid-solid interfaces of the plate leads to the global stiffness matrix K, which relates displacements (U_0, U_N) to stresses (T_0, T_N), subscripts 0 and N refer to the first and the last interface [25].

The characteristic equation for Lamb modes can be determined from the total stiffness matrix of the structure K or its inverse, the global compliance matrix S. If the top and bottom surfaces are free, the Lamb wave dispersion equation is determined as:

$$\det(K) = 0 \tag{6}$$

Complex solutions of Eq. (6) are now sought in order to predict the dispersion and attenuation curves in terms of frequencies. The Newton–Raphson is used to solve the nonlinear equations with complex coefficients. The real part $k_1^{'}$, of k_1, is related to the phase velocity of the mode by the classical relation Vph $V_{ph} = w/k_1^{'}$, while the imaginary part, i.e., $k_1^{''}$, represents its attenuation [26,27].

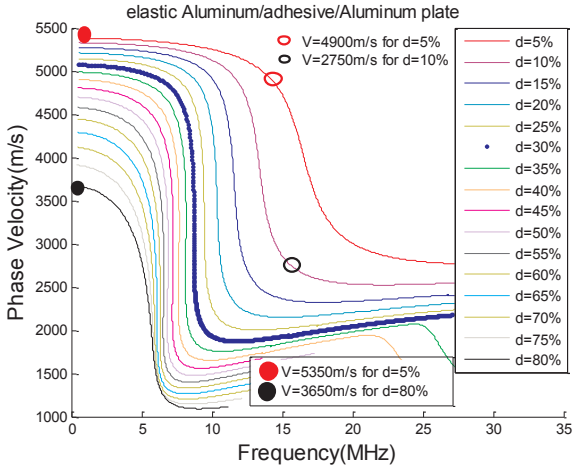

Fig. 4. The dispersion curves of the fundamental symmetric S_0 mode in the (phase velocity-frequency) plane, are calculated when the volumic fraction d of the thin Aluminum/adhesive/Aluminum plate varies from 5% to 80% in increments of 5%.

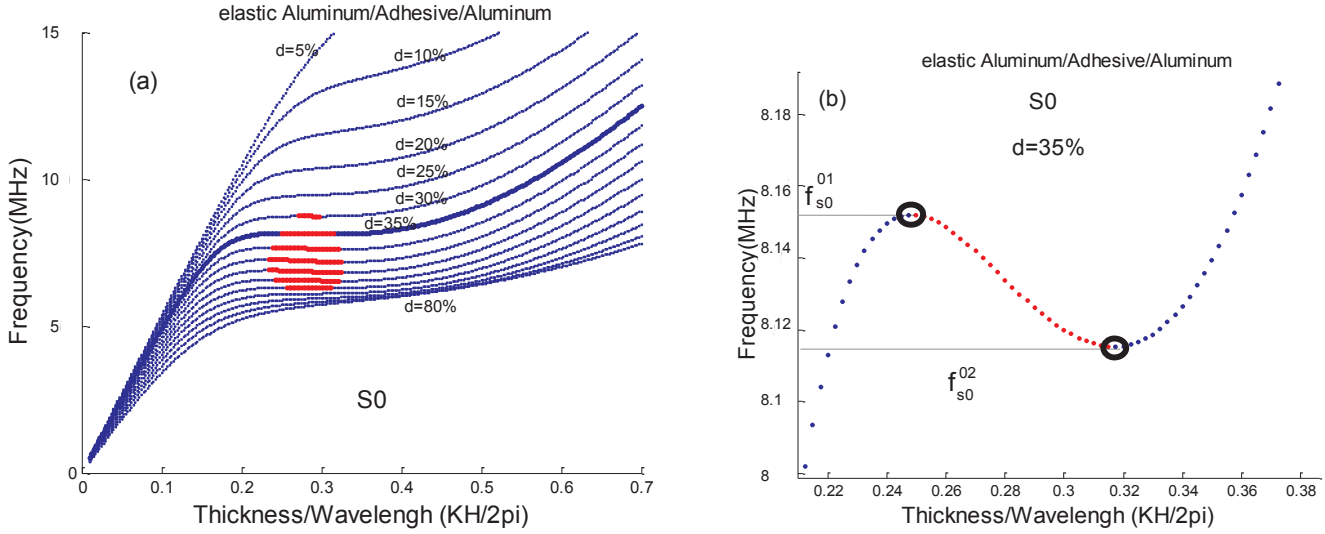

Fig. 5. The S_0 dispersion curve in the (frequency-thickness/wavelength) plane; for several values of volumic fraction d; red line: backward mode; blue line: forward mode; (b) S_0 dispersion curve for d = 35% around the frequency of the first S_0-ZGV mode (f_{s0}^{01}) and the second frequency of S_0-ZGV mode (f_{s0}^{02}). (For interpretation of the references to color in this figure legend, the reader is referred to the web version of this article.)

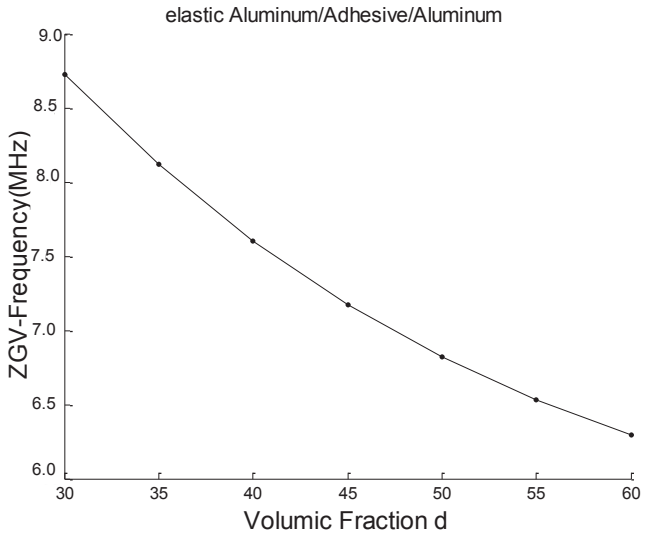

Fig. 6. The relationship between f_{s0}^{02} (the second frequency of S_0-ZGV mode) and the volumic fraction d.

3. Results and discussion

3.1. Validation of the approach by comparison with available data

Based on the previous formulations, a computer program with respect to the Stiffness matrix method has been written, using Matlab software, to calculate the dispersion and attenuation curves for a multilayer structure. In order to check the validity of the program, we deal with an example of a sandwich viscoelastic plate used in Ref. [28]. The sandwich structure is made of two anisotropic viscoelastic material skins, separated by a rigid, isotropic, viscoelastic core, designed for specific aerospace purpose. Fig. 2 shows the effect of material viscoelasticity on the dispersion and attenuation curves of the mode, labeled mode C, when $C_{ij}^{''}$ increases from 0.001% to 100% of their nominal values. It can be seen that our solutions are in good agreement with the published data, which are obtained from Transfer matrix method. In the case of an elastic 'glass-epoxy/foam/glass-epoxy plate, the phase velocity of several modes was calculated in Fig. 3(b). The agreement of our results is again obtained with those calculated by Casting.

3.2. Influence of volumic fraction of adhesive on the dispersion curves which have backward modes in elastic thin bonded Aluminum/adhesive/Aluminum plate

The fundamental modes S_0 and A_0 are the most commonly used modes for damage detection and material characterization, as compared to the higher-order modes [29]. In additional of the forward waves, the S_0 in the thin bonded plate can be present backward waves with double ZGV modes. In the aim to understand the relationship between the property change of the bonded plate and the different type of the guided waves, the influence of the volumic fraction d on the dispersion curve of the mode S_0 and its mode ZGV is studied. Thereafter, the influence of the volumic fraction on the forward mode, backward mode and their ZGV modes in S_1 and S_2 modes are investigated.

3.2.1. Influence of adhesive layer thickness on S_0 mode in elastic symmetric bonded Aluminum/Adhesive/Aluminum plate

The thin bonded plate Aluminum/adhesive/Aluminum having a thickness of 100 μm. It is composed of two identical, isotropic, and homogeneous aluminum plates joined together with an adhesive bonding layer. The three component layers of the plate have of thickness h_k (k = 1, 2, 3) Fig. 1(b). Their material properties are those noted by Hong-Xiang et al. [1] given in Table1. To investigate the influence of the volumic fraction d on the phase velocity of the fundamental symmetric mode, the S_0 dispersion curves in the (frequency-phase velocity) plane, are calculated when d varies from 5% to 80% in increments of 5% Fig. 4. It can be observed the increasing of the phase velocities when d decreases. In the range of lower frequency, where the S_0 mode is slightly dispersive the phase velocity is varied from V = 3650 ms^{-1} for d = 80% to V = 5350 ms^{-1} for d = 5%, and the sensitivity of the phase velocity to the thickness of the adhesive layer increases as d increases. However, in the zone which is strongly dispersive, the phase velocity of S_0 mode becomes increasingly sensitive to the change in adhesive thickness when d decreases. For example, at the frequency f = 15 MHz the phase velocity is varied from V = 2750 ms^{-1} for d = 10% to V = 4900 ms^{-1} for d = 5%. Therefore, for a bonded plate characterized by a low value of volumic fraction d, the determination of this dispersion curve region may be useful for obtaining information on the adhesive layer.

To better see the appearance of the backward mode, for which the energy velocities of the waves are negative, the S_0 dispersion curve is

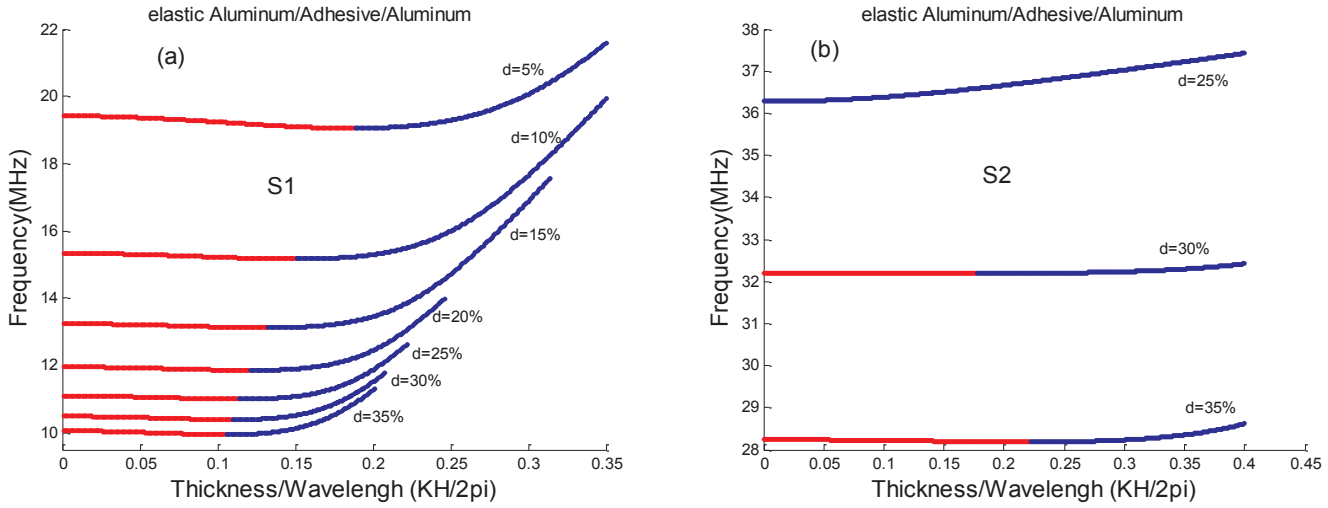

Fig. 7. The impact of volumic fraction change on the dispersion curves of: (a) S_1 mode and (b) S_2 mode; red line: backward mode; blue line: forward mode. (For interpretation of the references to color in this figure legend, the reader is referred to the web version of this article.)

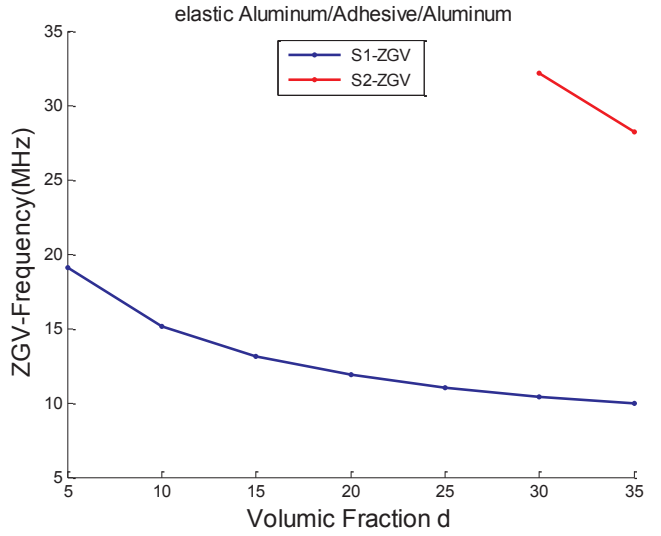

Fig. 8. The relationship between volumic fraction d and: frequency of S_1-ZGV mode f_{s1}^0 (blue line); and frequency of S_2-ZGV mode $f_{s_2}^0$ (red line). (For interpretation of the references to color in this figure legend, the reader is referred to the web version of this article.)

plotted in the (frequency f – thickness/wavelength $kH/2\pi = H/\lambda$) plane Fig. 5(a). The ZGV modes correspond to the points where the slopes are parallel to the axis of the kH-axis, and the backward mode corresponds to the points at which the slopes are negatives. In Fig. 5, the backward mode is plotted as red line and the forward mode as blue line. Between them, we found the ZGV mode, for $d > 25\%$, two ZGV modes occurs in the dispersion zone of the S_0 curve. Thus, the increase of d caused the appearance of double ZGV mode for S_0 (double S_0-ZGV mode). As an example, for $d = 35\%$, there are two frequencies say $f_{s_0}^{01}$, $f_{s_0}^{02}$, on the frequency axis for which the group velocity is zero Fig. 5(b). In the interval $[f_{s_0}^{01}, f_{s_0}^{02}]$, phase and group velocities are of opposite signs: backward wave occurs. It is plotted as red line in Fig. 5(b). The frequencies of S_0-ZGV mode say $f_{s_0}^{02}$ has been plotted for several volumic fraction d in Fig. 6. Investigating this curve it can be seen that in the volumic fraction intervals of [30–60%], the frequency of S_0-ZGV mode decreases with an increase of d. Thereafter, The S_0-ZGV mode disappears when the volume fraction d becomes greater than 60%.

3.2.2. *Influence of adhesive layer thickness on S_1 and S_2 modes in elastic bonded Aluminum/Adhesive/Aluminum plate*

In the goal to see the influence of the adhesive layer thickness on the backward and the forward modes in the symmetric modes, the dispersion curves of S_1 and S_2 are plotted for several values of d Fig. 7, the backward mode is plotted as red line and the forward mode as blue line. Between these two modes we find the ZGV mode. For S_1 mode, we can observe that the length of the branch of the backward mode increases as d decreases. Unlike the case of S_2 mode, the length of the backward mode decreases as d decreases, and it no longer exists from $x = 25\%$. for the both symmetric modes S_1 and S_2, the region of the curve where the modes are strongly dispersive, are sensitive to change of d. this sensitivity of the forward and backward mode to middle layer thickness, becomes clearer in the case of a plate having a thinner thickness of adhesive. Fig. 8 shows the dependence of the frequency f_{S1}^0 of S_1-ZGV mode; and the dependence of the frequency f_{S2}^0 of S_2-ZGV mode, on the volumic fraction d. One can see that the frequencies f_{S1}^0 and f_{S2}^0 decrease when d increase.

3.3. *Effect of viscous adhesive layer thickness on the Lamb modes which have ZGV modes*

Complex solutions of dispersion equations Eq. (6) are now sought to quantify the viscous effects on dispersion curves that have ZGV modes. The effects of volume fractions d of adhesive on damped modes have been studied.

3.3.1. *Connection between the symmetric S_0, S_1 and S_2 modes: Particular case $d = 35\%$*

For the case of bonded plate with volumic fraction $d = 35\%$, Fig. 9 shows that at the frequencies of ZGV modes (frequency of second S_0-ZGV mode (S_0-ZGV2), frequency of S_1-ZGV mode, and frequency of S_2-ZGV mode), the viscous property of the bonded plate gives rise to a phenomenon of connections between the dispersion curves of S_0, S_1 and S_2 modes. The attenuation curve of the coupling mode, which is labeled as mode C, shows that these coupling phenomena correspond to a relatively high attenuation level Fig. 9(b). The backward mode, which is located between the two S_0-ZGV frequencies: $f_{S_0}^{01}$ and $f_{S_0}^{02}$, disappeared when one takes into account the material viscoelasticity. And another mode labeled F appeared with mode C Fig. 9(a). To compare the attenuation coefficients $K''_{S0-ZGV1}$ and $K''_{S0-ZGV2}$ of the first and second S_0-ZGV modes respectively, the attenuations curve of modes C and F are plotted together in the same figure Fig. 9(c) around the frequency $f_{S_0}^{02} = 8.15$ MHz. The attenuation coefficient $K''_{S0-ZGV2}$ of the second S_0-

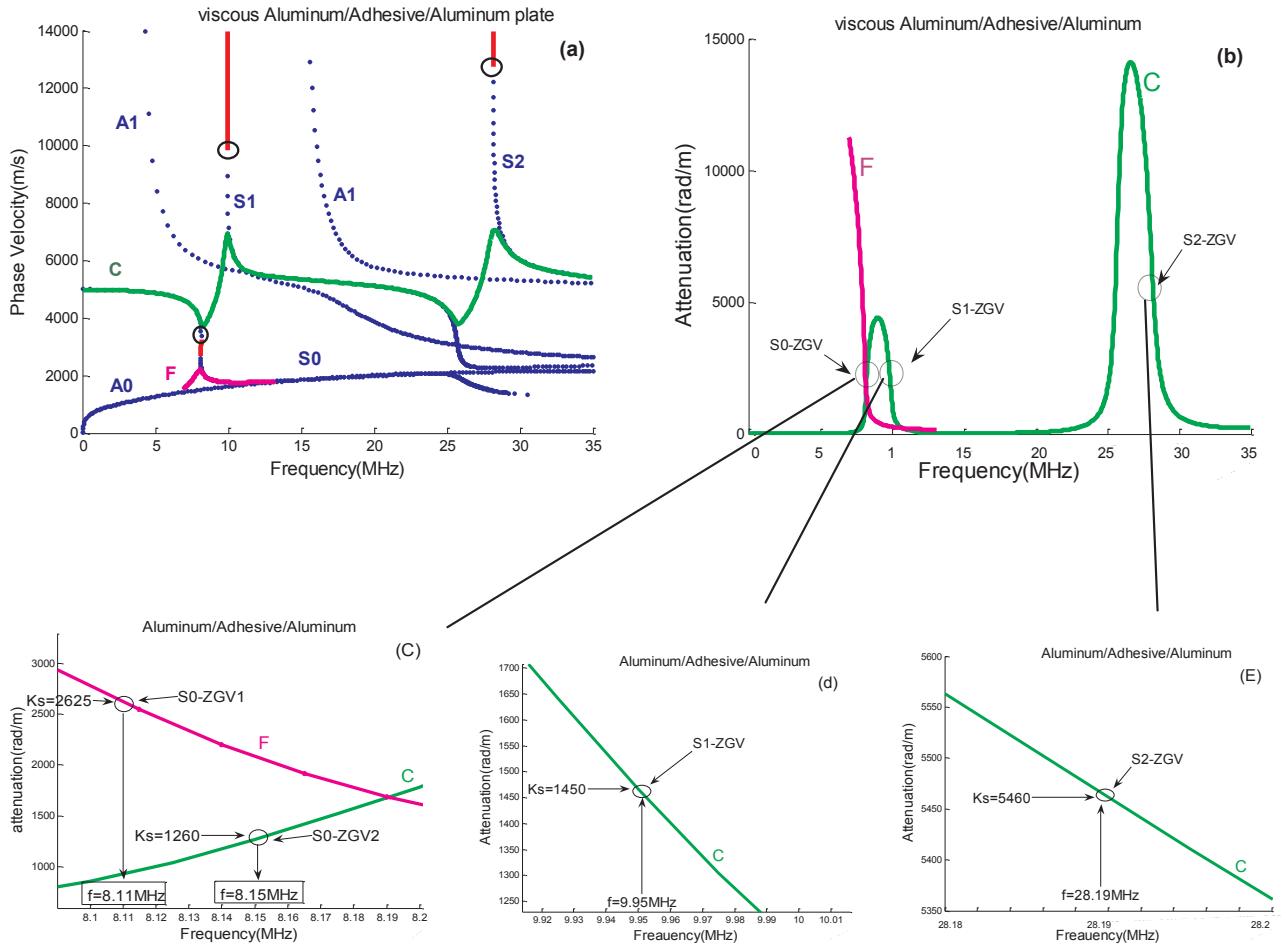

Fig. 9. Coupling phenomenon between symmetric modes in the viscous bonded plate Aluminum/Adhesive/Aluminum: case of the volumic fraction of adhesive d = 35%; (a) blue line: the dispersion curves in the elastic plate and the others colors are the curves in viscous plate; (b) the attenuation curve of mode C and mode F; for the clarity of the numerical values of the ZGV mode's attenuation coefficients, three zoom of the attenuation curve are plotted around of: (c) frequencies of B-ZGV; (d) frequency of d-ZGV mode; and (e) frequency of E-ZGV mode. (For interpretation of the references to color in this figure legend, the reader is referred to the web version of this article.)

ZGV mode is determined from the attenuation curve of C mode at the S_0-ZGV1 mode's frequency $f_{S_0}^{02} = 8.15$MHz.: $K''_{S0-ZGV2} = 1260$ rad m^{-1}. At the frequency $f_{S_0}^{01} = 8.11$ MHz, the attenuation curve of mode F exhibits the attenuation coefficient $K''_{S0-ZGV1}$ of the first S_0-ZGV mode: $K''_{S0-ZGV1} = 2625$ rad m^{-1}. It is approximately two times greater than the attenuation coefficient of the S_0-ZGV2 mode. Indeed, in the viscous plate, the energy velocity of the quasi-ZGV mode is slightly different from zero. The guided waves are attenuated exponentially, and then these values of the attenuation coefficients lead to large differences between the amplitudes decrease of these modes during the propagation, even along a short propagation distance. The zoom of the attenuation curve of the coupling mode C around of $f_{s1}^0 = 9.95$ MHz and $f_{s2}^0 = 28.19$ MHz Fig. 9(d), show that the values of the attenuation coefficients of S_1-ZGV mode and S_2-ZGV mode are: $K''_{S1-ZGV} = 1460$ rad m^{-1} and $K''_{S2-ZGV} = 5460$ rad m^{-1}, respectively.

3.3.2. Comparison between real and complex solutions of the dispersion equation for several values of d

In order to study the influence of the volumic fraction d on the symmetric S_0, S_1 and S_2 modes; which their dispersion curves may exhibit ZGV modes, the real and complex solutions of the dispersion equation are plotted together in the same figure Fig. 10. The dispersion curves in the elastic plate are plotted in blue lines. The dispersion and attenuation curves in the viscous plate are plotted in a green and mauve lines. Phenomena of connection between S_0, S_1 and S_2 modes at the frequencies of ZGV modes f_{S0}^{02}, f_{S1}^0 and f_{S2}^0 are investigated for many thin bonded plate. Of the three-layer of the thin bonded plate, only the adhesive layer is considered to be viscous. It is therefore obvious that the increase in the volumic fraction d of the adhesive leads to an increase in the level of the viscoelastic properties of the bonded plate, which is at the origin of the coupling phenomenon. This explains the increase in the number n of the symmetric modes which coupling together when d increases Fig. 10.

For d ≤ 15%, n = 0 and the dispersion curves are unchanged whether real or complex solutions are sought Fig. 10(a), (c) and (e), with the exception of the backward mode (in the spectrum of S_1 mode) which no longer exists. For d = 20%, S_0 does not have a ZGV mode yet. And the two dispersion curves of the modes S_0 and S_1 connect together at the frequency of S_1-ZGV mode Fig. 10(g). For d = 25%, the two dispersion curves of the modes S_0 and S_1 connect together at the frequency of S_0-ZGV2 mode and at frequency of S_1-ZGV mode Fig. 10(i). However, from d = 30%, n = 3; we can see the connection between the three symmetric modes S_0, S_1 and S_2; at the frequencies of S_0-ZGV2, S_1-ZGV and S_2-ZGV modes Fig. 10(k) and (m). For the all values of d, the dispersion and attenuation curves in the Fig. 10 show that both the zone of strong dispersion and the zone where the coupling phenomenon occurs, correspond to high attenuation levels.

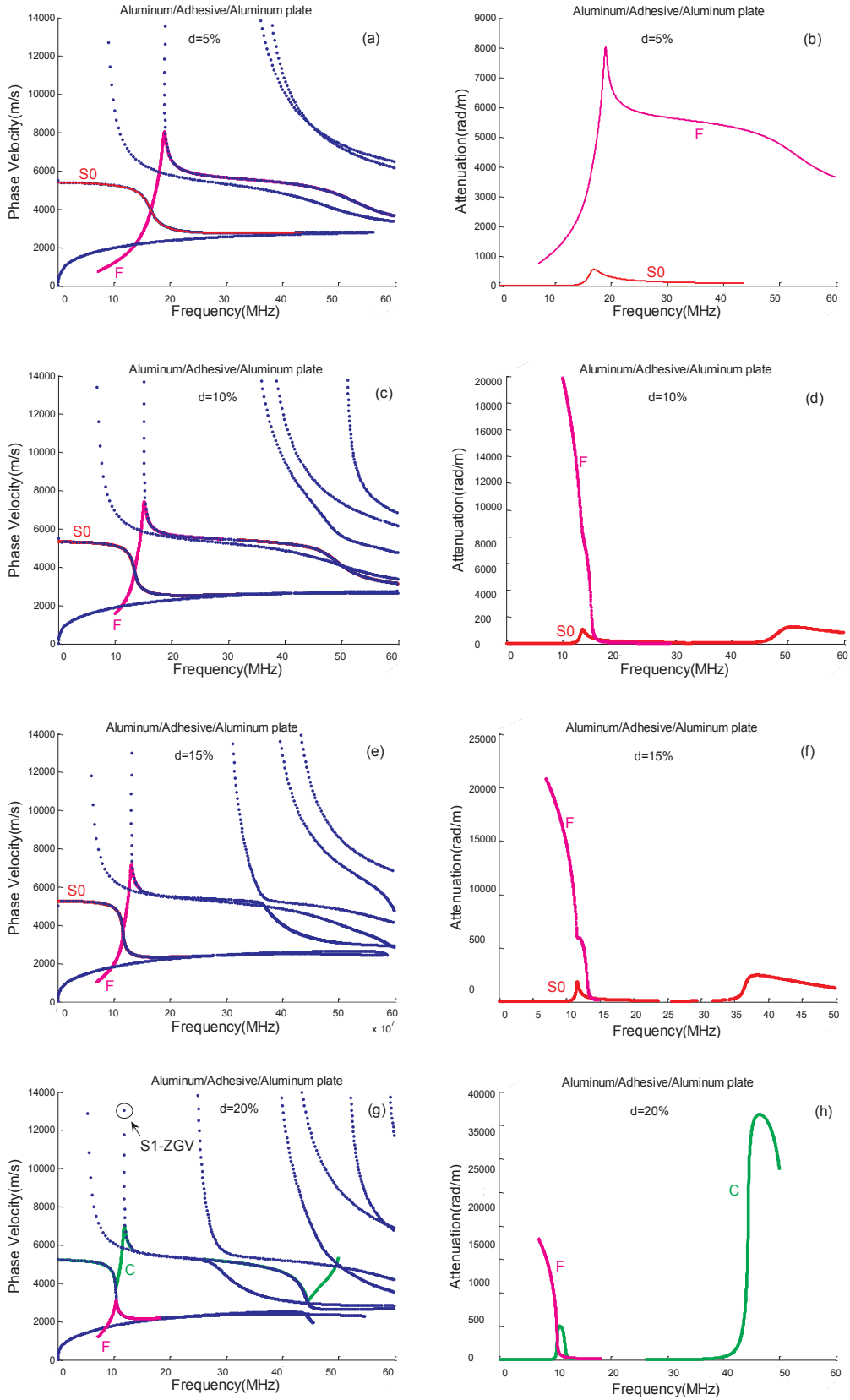

Fig. 10. The influence of the volumic fraction d on real solution (blue line) and on complex solutions (the others colors); The dispersion curves: (a) for d = 5%, (c) for d = 10%, (e) for d = 15%; (g) for d = 20%; (I) for d = 25%; (k) for d = 30%; (m) for d = 35%; The attenuation curves of the modes in viscous plates are plotted in: (b) for b = 5%, (b) for d = 10%, (f) for f = 15%, (h) for h = 20%, (j) for = 25%, (l) for b = 30%, (n) for b = 35%. (For interpretation of the references to color in this figure legend, the reader is referred to the web version of this article.)

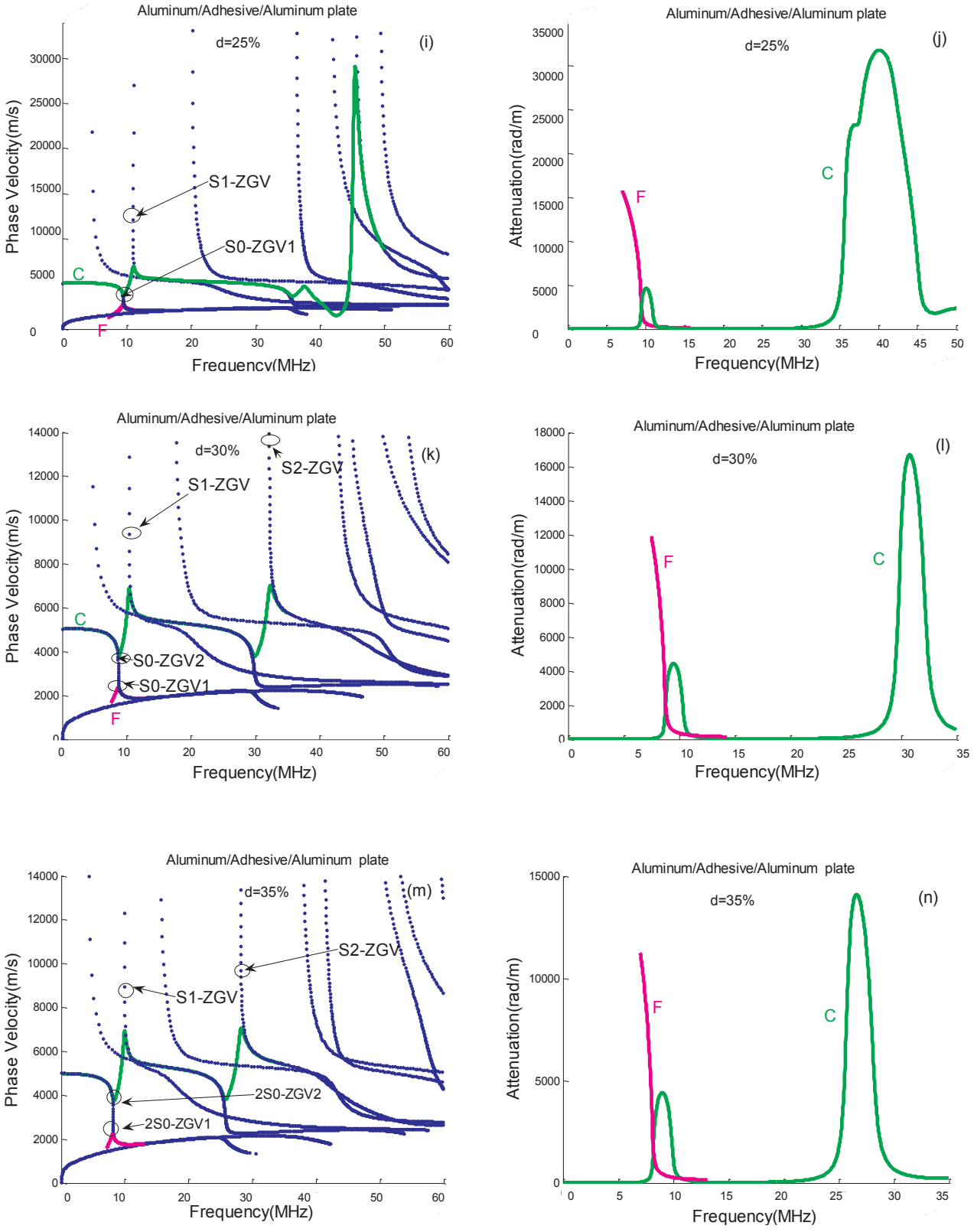

Fig. 10. (*continued*)

3.3.3. Effect of viscous adhesive layer thickness on the fundamental S_0 mode

To better see the evolution of damped fundamental S_0 mode when d increases, the dispersion and attenuation curves of S_0 mode and F mode are plotted for several values of the volumic fraction d in Fig. 11. For the clarity of the attenuation level of S_0 when d = 15%, 10% and 5%, a zoom of Fig. 11(b) is shown in Fig. 11(c). As we have seen previously in Section 3.2.1, the S_0 phase velocities are strongly sensitive to the change in the thickness of the thin adhesive layer when d decreases. Moreover, Fig. 11(c) shows that S_0 attenuation level decreases when the

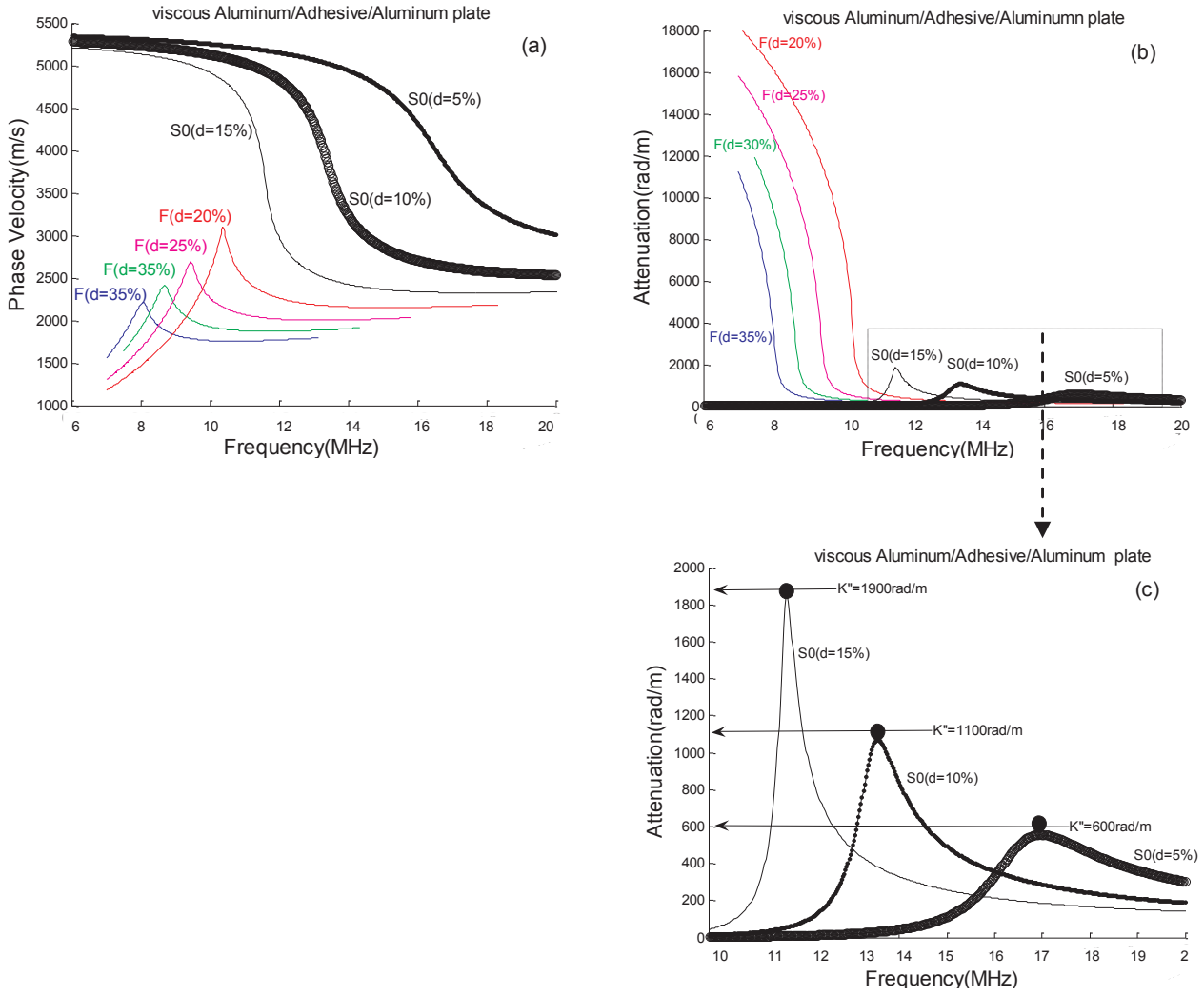

Fig. 11. Influence of viscous property on S_0 mode; (a) dispersion curve; (b) attenuation curve; When d increases, S_0 disappears and F mode appears. This F mode is strongly attenuate. (c) a zoom of Fig. 11(b) to better show the attenuation level of S_0 mode for d = 5%, 10 and 15%.

volumic fraction d decreases. For d = 5%, d = 10% and d = 15%, the points correspond to the maximum of S_0 attenuation coefficient are indicated by * in Fig. 11(c), their values are K''_{S0Max} = 1900 rad/m and K''_{S0MAX} = 1100 rad/m, and K''_{S0MAX} = 600 rad/m, respectively. When d decreases, the phase velocity of S_0 mode becomes more sensitive to d change. Moreover, S_0 mode becomes less attenuated. Therefore, in the case of bonded plates which have a small adhesive layer thickness, this fundamental mode S_0 can be used in the inspection service of the characteristic of the thin adhesive layer. However when the volumic fraction d increases, e.i. for d ≥ 20%, the S_0 mode disappeared and the mode F occurs with very high attenuation level Fig. 11(b). Therefore, mode F can be considered as evanescent mode [26].

3.3.4. *Effect of viscous adhesive layer thickness on coupling mode between S_0 and S_1 modes*

Around the frequencies of S_0-ZGV mode and S_1-ZGV mode, the dispersion and attenuation curves of S_0 mode and S_1 mode are plotted for several values of volumic fraction d in Fig. 12. For d ≤ 15%, the viscous properties cannot give rise to coupling phenomena between S_0 mode and S_1 mode Fig. 12(a), and the S_1 mode is characterized by a high attenuation level below the frequency of S_1-ZGV mode Fig. 12(b) (the ZGV modes are indicated by o). For d = 20% and d = 25%, the high level of the plate viscoelastic property gives rise to coupling phenomenon between the dispersion curve of S_0 mode and the dispersion curve of S_1 mode at the frequency of S_1-ZGV mode. For d > 25%, double ZGV mode appears in the S_0 dispersion curve, and the viscoelastic property gives rise to coupling phenomenon between the dispersion curve of S_0 mode and the dispersion curve of S_1 mode, at the frequency of S_0-ZGV2($f_{S_0}^{02}$) mode and the frequency of S_1-ZGV mode. So a single curve is obtained, and forming the dispersion curve of C mode. It can be observed that the increase in d caused the shift of dispersion and attenuation curves toward the decreasing direction of the frequency axis, without significant change in the values of the phase velocity of the C coupling mode.

From the attenuation curves, it can be seen that the C coupling mode is less attenuated when the thickness of the viscous adhesive layer increases. Therefore in this frequency range, the sensitivity of the coupling mode C as well as their diminishingly attenuate coefficients when the adhesive layer thickness d increases, makes it suitable for the detection of the properties changes in the high damping bonded plate.

Fig. 12(c) and (d) gives the attenuation level of the S_0-ZGV2 (mode second S_0-ZGV mode) and the attenuation level of S_1-ZGV modes. The values of the frequency and attenuation coefficients of S_0-ZGV2 mode and S_1-ZGV mode for different values of volumic fraction d are given in Table2. This table reveals that the attenuation coefficients of S_1-ZGV mode diminishes from 2215 rad m^{-1} to 1465 rad m^{-1}, as the viscoelastic property increases, i.e. when the volumic fraction of adhesive increases from d = 5% to d = 35%. In addition, for d = 30% the

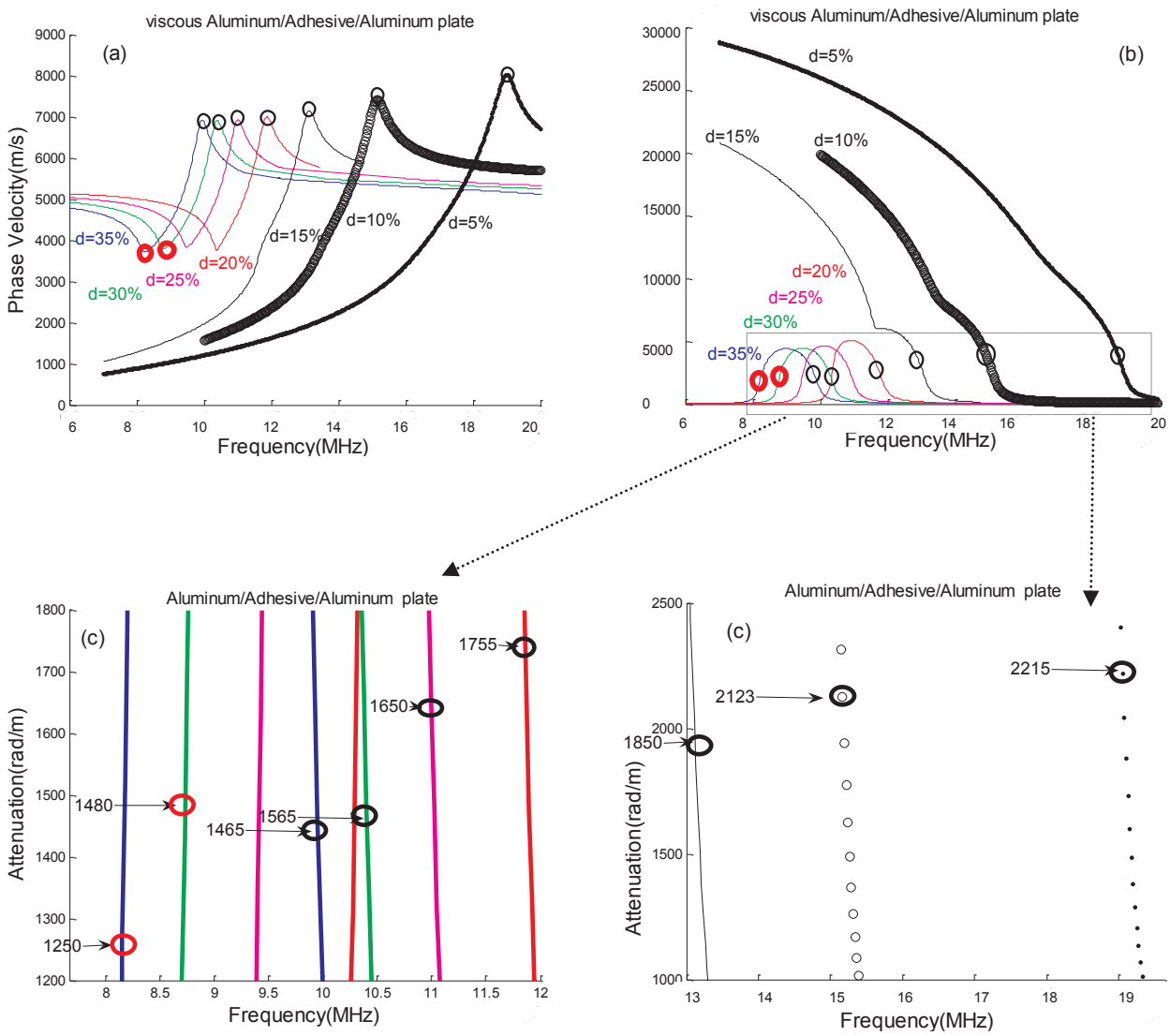

Fig. 12. The dispersion (a) and attenuation (b) curves of the symmetric modes around the frequencies of S0-ZGV mode and S1-ZGV mode. (c): zoom of the C attenuation curve around the frequencies of ZGV modes. (d): zoom of the S1 attenuation curve around the frequency of S1-ZGV mode. The attenuation coefficient $K''_{S0-ZGV2}$ at the frequency of S_0-ZGV2 mode is indicate by O; and the attenuation coefficient K''_{S1-ZGV} at the frequency of S_1-ZGV mode is indicate by O.

Table 2
The attenuation coefficient $K''_{S0-ZGV2}$ of second ZGV mode (S_0-ZGV2 mode); And the attenuation coefficient K''_{S1-ZGV} of S_1-ZGV mode; for several values of volumic fraction d.

	$f^{02}_{S_0}$ (MHz)	$K''_{S0-ZGV2}$ (rad m^{-1})	$f^{0}_{S_1}$ (MHz)	K''_{S1-ZGV} (radm^{-1})
d = 35%	8.15	1250	9.95	1465
d = 30%	8.73	1480	10.39	1565
d = 25%	no S0-ZGV mode	–	11	1650
d = 20%	no S0-ZGV mode	–	11.86	1755
d = 15%	no S0-ZGV mode	–	13.14	1850
d = 10%	no S0-ZGV mode	–	15.17	2123
d = 5%	no S0-ZGV mode	–	19.05	2215

difference between the attenuation coefficients $K''_{S0-ZGV2}$ and K''_{S1-ZGV} is 1565–1480 = 85 rad/m. For d = 35%, $K''_{S1-ZGV} - K''_{S1-ZGV}$ is 1465–1250 = 215 rad/m. Therefore, there is an increase in the difference between the attenuation level of the S_0-ZGV mode and the S_1-ZGV mode, when d increases from d = 30% to 35%.

3.3.5. *Effect of viscous adhesive layer thickness on coupling mode between C and S_2 modes*

To investigate the influence of volumic fraction d on the coupling phenomena between C mode and S_2 mode, their dispersion and attenuation curves are plotted around the frequency of S_2-ZGV mode in Fig. 13, for several values of d in the same figure. As in the case of the first coupling between S_0 and S_1 modes, the attenuation level of the coupling mode C decreases as the plate viscoelasticity property

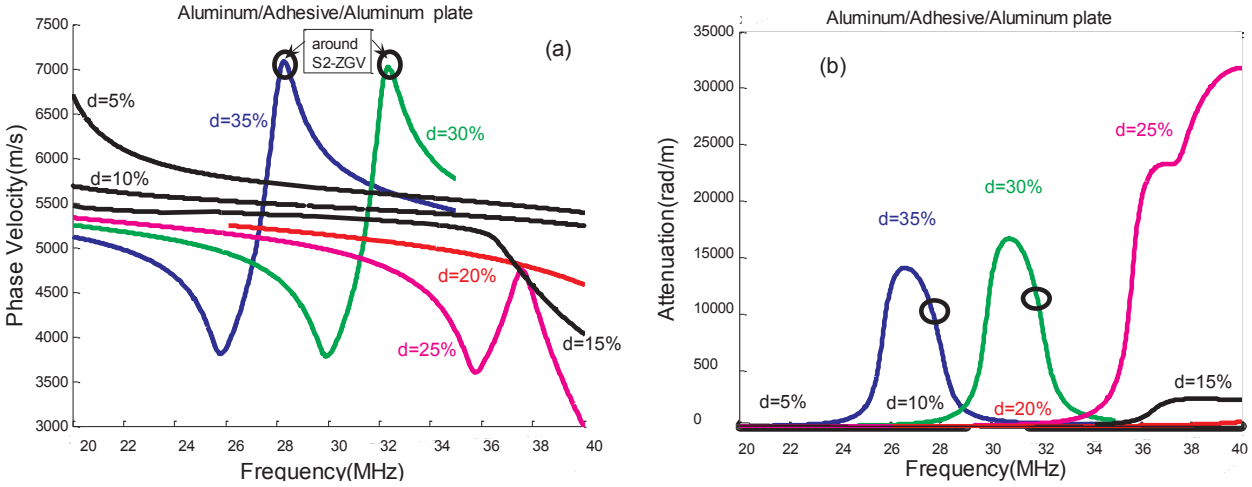

Fig. 13. The dispersion (a) and attenuation (b) curves of C mode in viscous plate around the frequency of S_2-ZGV mode (indicate by O), for several volumic fraction d.

increases. For d = 35% and d = 30% we can see the coupling between C and S_2 at the frequency of S_2-ZGV mode. It can be observed that the increase in d caused the shift of dispersion and attenuation curves toward the decreasing direction of the frequency axis, without significant change in the values of the phase velocity, and with slight decreases in the attenuation level of the C coupling mode. For d ≤ 25%, the coupling phenomena no longer exist. Recalling that, in the elastic plate, the dispersion curve of S_2 mode no longer has ZGV mode for d ≤ 25% Fig. 7(b).

4. Conclusion

The Stiffness method is used to calculate the dispersion and attenuation curves in thin bonded plate, which characterized by the strongly different acoustic impedances between their layers.

The sensitivity of the phase velocity of the symmetric mode to the variation of the thickness h of the elastic adhesive layer in a three-layer plate with Aluminum/Adhesive/Aluminum configuration has been studied. The study was carried out when the total thickness of the plate remain constant and equal to 100 µm. For the low value of volumic fraction d (d = 10%, 5%), it has been observed that the phase velocity in the dispersive zone is very sensitive to change in thickness of the adhesive layer. However, the non-dispersive zone is sensitive to the change in the thickness of the thick adhesive layer (d = 60%, 55%…). The increase of d caused the appearance of double ZGV modes for S_0. The frequency of S_0-ZGV mode decreases with an increase of d. The large differences between stiffness tensors of the skin and the adhesive, as well as the value of the volumic fraction d, seem to be the causes of this local resonance in the fundamental mode. For S_1 mode, the length of the branch of the backward mode increases as d decreases. Unlike the case of S_2 mode, the length of the branch of the backward mode decreases as d decreases. When d decreases the backward mode in the S_2 spectrum no longer exists for d ≤ 25%. For the both symmetric modes S_1 and S_2, the region of the curve where the modes are strongly dispersive is very sensitive to change of d. The frequencies of S_1-ZGV and S_2-ZGV modes decrease when d increases. At the frequencies of ZGV modes (frequency of second S_0-ZGV mode (S_0-ZGV2 mode), frequency of S_1-ZGV mode, and frequency of S_2-ZGV mode), the viscous property of the bonded plate gives rise to a phenomenon of connections between the dispersion curves of S_0, S_1 and S_2 modes. The backward mode disappeared when one takes into account the material viscoelasticity and a coupling mode appears. The influence of the volumic fraction d in the dispersion and attenuation curves of the coupling mode C is investigated. The frequency range around each frequency of ZGV mode, where the coupling phenomenon occurs, corresponds to high attenuation levels. Attenuation level of S_0 mode decreases when the volumic fraction d decreases. From d = 20%, the S_0 mode disappeared and the mode C occurs with very high attenuation level around the S_1-ZGV frequency. In the range between the frequencies of S_0-ZGV2 mode and the frequency of S_1-ZGV mode it is observed that the increase in d caused the shift of dispersion and attenuation curves toward the decreasing direction of the frequency axis, without significant change in the values of the phase velocity of the C coupling mode. The attenuation coefficients of S_0-ZGV2 mode and S_1-ZGV mode for different values of volumic fraction d are calculated. The attenuation coefficients decrease when d increases. When d increases, ZGV mode appears in dispersion curve of S_2 mode, and coupling phenomena occurs between dispersion curve of C mode and dispersion curve of S_2 mode at the frequency of S_2-ZGV mode. Around the frequency of S_2-ZGV mode, it is observed that the increase in d caused the shift of C dispersion and attenuation curves toward the decreasing direction of the frequency axis, without significant change in the values of the phase velocity, and with slight decreases in the attenuation level of the C coupling mode.

Appendix A. Supplementary material

Supplementary data to this article can be found online at https://doi.org/10.1016/j.ultras.2018.12.005.

References

[1] S. Hong-Xiang, X. Bai-Qiang, Z. Hua, G. Qian, Z. Shu-Yi, Influence of adhesive layer properties on laser-generated ultrasonic waves in thin bonded plates, Chin. Phys. B 20 (1) (2011) 014302.
[2] P. Fromme, P.D. Wilcox, M.J.S. Lowe, P. Cawley, On the development and testing of a guided ultrasonic wave array for structural integrity monitoring, IEEE Trans. Ultrason. Ferroelectr. Freq. Control 777 (2006) 785–853.
[3] D.N. Alleyne, P. Cawley, The interaction of Lamb waves with defects, IEEE Trans. Ultrason. Ferroelectr. Freq. Control 381 (1992) 397–439.
[4] M. Castaings, E. Le Clezio, B. Hosten, Modal decomposition method for modeling the interaction of Lamb waves with cracks, J. Acoust. Soc. Am. (2002) 112-2567-2582.
[5] Bernard M, Christian R, Paul F. High-frequency guided ultrasonic waves for hidden defect detection in multi-layered aircraft structures. Ultrasonics 2014; ULTRAS 4824 No. of Pages 9, Model 5G.
[6] H. Cho, Y. Yaguchi, H. Ito, Characterization of the bond quality of adhesive plates utilizing zero-group-velocity Lamb waves measured by a laser ultrasonics technique, Jpn. Soc. Mech. Eng. (2014) J-STAGE Advance Publication date: 11, 2014.
[7] D. Clorennec, C. Prada, D. Royer, Laser ultrasonic inspection of plates using zero-group velocity Lamb modes, IEEE Trans. Ultrason. Ferroelectr. Freq. Control 57 (5) (2010) 1125–1132.
[8] H. Cho, Y. Hara1, T. Matsuo, Evaluation of the thickness and bond quality of three-layered media using zero-group-velocity lamb waves, J. Phys.: Conf. Ser. 520 (2014) 012023.
[9] K. Nishimiya, K. Mizutani, N. Wakatsuki, K. Yamamoto, Relationships between existence of negative group velocity and physical parameters of materials for Lamb-

type waves in solid/liquid/solid structure, Jpn. J. Appl. Phys. 47 (2008) 3855–3858.
[10] Clemens M. Grünsteidl, Todd W. Murrayb, Istvan A. Veresa, Numerical investigation of the excitability of zero group velocity lamb waves, in: 2015 International Congress on Ultrasonics, 2015 ICU Metz Physics Procedia 2015, vol. 70, p. 159–162.
[11] S. Mezil, J. Laurent, D. Royer, C. Prada, Non contact probing of interfacial stiffnesses between two plates by zero-group velocity Lamb modes, Appl. Phys. Lett. 105 (2014) 021605.
[12] S. Rokhlin, Y. Wang, Analysis of boundary conditions for elastic wave interaction with an interface between two solids, J. Acoust. Soc. Am. 89 (1991) 503–515.
[13] J.P. Jones, J.S. Whittier, Waves at a flexibly bonded interface, J. Appl. Mech 34 (1967) 905–909.
[14] M. Sylvain, B. Francois, R. Samuel, J. Laurent, R. Daniel, P. Claire, Investigation of interfacial stiffnesses of a tri-layer using Zero-Group Velocity Lamb modes. arXiv: 1511.04367v1 [cond-mat.mtrl-sci] 13 November 2015.
[15] M.V. Predoi, Guided waves dispersion equations for orthotropic multilayered pipes solved using standard finite elements code, Ultrasonics 54 (2014) 1825-1831.
[16] M.J.S. Lowe, D.N. Alleyne, P. Cawley, Defect detection in pipes using guided waves, Ultrasonics 36 (1998) 147–154.
[17] H. Cui, W. Lin, H. Zhang, X. Wang, Backward waves with double zero-group-velocity points in a liquid-filled pipe, J. Acoust. Soc. Am. 139 (3) (2016) 1179–1194.
[18] T. Hussain, F. Ahmad, Lamb modes with multiple zero-group velocity points in an orthotropic plate, Acoust. Soc. Am. 132 (2) (2012) 641–645.
[19] A.A. Maznev, A.G. Every, Surface acoustic waves with negative group velocity in a thin film structure on silicon, Appl. Phys. Lett. 95 (2009) 011903.
[20] B. Hosten, M. Castaings, Transfer matrix of multilayered absorbing and anisotropic media: measurements and simulations of ultrasonic wave propagation through composite materials, J. Acoust. Soc. Am. 94 (1993) 1488–1495.
[21] B. Hosten, M. Castaings, Delta operator technique to improve the Thomson-Haskell method stability for propagation in multilayered anisotropic absorbing plates, J. Acoust. Soc. Am. 95 (1994) 1931–1941.
[22] S. Pant, J. Laliberte, M. Martinez, B. Rocha, Derivation and experimental validation of Lamb wave equations for an n-layered anisotropic composite laminate, Compos. Struct. 111 (2014) 566–579.
[23] Pezhman TB, Khosro NT, Sina S, Mohammad S. Investigation of Lamb waves attenuation in elastic–viscoelastic three-layer adhesive joints in low and high frequencies: theoretical modeling, in: Proc IMechE C: J. Mech. Eng. Sci. 2014. p. 1–14.
[24] S.I. Rokhlin, L. Wang, Stable recursive algorithm for elastic wave propagation in layered anisotropic media: Stiffness matrix method, J. Acoust. Soc. Am. 112 (2002) 822–834.
[25] S.I. Rokhlin, L. Wang, Ultrasonic waves in layered anisotropic media: characterization of multidirectional composites, Int. J. Solids Struct. 39 (2002) 5529–5545.
[26] S. Dahmen, M. Ben Amor, M.H. Ben Ghozlen, Investigation of the coupled Lamb waves propagation in viscoelastic and anisotropic multilayer composites by Legendre polynomial method, Compos. Struct. 153 (2016) 557–568.
[27] S. Dahmen, H. Ketata, M.H. Ben Ghozlen, Elastic constants measurement of anisotropic Olivier wood plates using air-coupled transducers generated Lamb wave and ultrasonic bulk wave, Ultrasonics 50 (2010) 502–507.
[28] M. Castaings, B. Hosten, Guided waves propagating in sandwich structures made of anisotropic, viscoelastic, composite materials, J. Acoust. Soc. Am. 113 (2003) 2622–2634.
[29] S. Pant, J. Laliberte, M. Martinez, B. Rocha, D. Ancrum, Effects of composite lamina properties on fundamental Lamb wave mode dispersion characteristics, Compos. Struct. 124 (2015) 236–252.